

PACS numbers: 87.64.Cc; 87.64.kp; 87.85.–d
DOI: 10.1070/QE2014v044n07ABEH015546

Raman spectroscopy of the organic and mineral structure of bone grafts

E.V. Timchenko, P.E. Timchenko, L.T. Volova, Yu.V. Ponomareva, L.A. Taskina

Abstract. **We report the results of experimental Raman spectroscopy of donor bone samples (rat, rabbit and human) with varying degrees of mineralisation. Raman spectra are obtained for the Raman bands of 950–962 cm^{-1} $(PO_4)^{3-}$, 1065–1070 cm^{-1} $(CO_3)^{2-}$ and 1665 cm^{-1} (amide I). In demineralised bone, a sharp (98%) decrease in the intensities of 950–962 and 1065–1070 cm^{-1} bands is observed, which is accompanied by the emergence of the 1079–1090 cm^{-1} band corresponding to the hydrated amorphous state CO_3^{-3}.**

Keywords: *Raman scattering, graft, demineralisation, spectrum.*

1. Introduction

A continual increase in global demand for bone graft materials is due to high rates of traumatic fractures [1]. Despite its initial ability to regenerate, bone tissue loses its properties during metabolic disorder and mineralisation of the bone matrix that eventually leads to the need for bone grafts [2]. This raises a number of problems associated with introduction of biomaterials directly into the body: disruption of homeostasis, implant rejection and its poor integration.

Of particular importance in the successful solution of these problems are physical methods for control of bone graft engineering. The commonly used methods, e.g. FTIR spectroscopy, allow one to register the mineral components of bone tissue, but do not make it possible to distinguish between the types of minerals that make up the crystal lattice of the mineral in question [3].

Bone grafts should fill the bone defect without causing immunological rejection and have biological activity, sterility and biodegradability, i.e., gradual replacement of bone defects [4]. The known technique is to provide a bone biomaterial for transplantation by means of demineralisation of bone tissue (it increases its regenerative function up to 90% [5]) which, by the end of the process, retains less than 5% of the calcified substance [4]. The authors [6] noted the presence of osteoinductive activity of completely and partially demineralised bone biomaterial, with highest activity being observed in the latter case. Incompleteness of demineralisation is explained by a strong bond of an osteoinductor (organic component), responsible for bone formation, with the mineral component of bone tissue [7]. Acquisition of information about the mineral component is of particular importance for cell cultures, such as osteoblasts [8].

Biomineralisation was assessed from the angular change in the intensity of diffracted X-ray radiation using the Debye–Scherrer powder method [9, 10]. The authors of [11, 12] suggested using the methods of Raman spectroscopy to determine the composition of the mineral component of bone material. In order to increase the regenerative functions of bone tissue, it is necessary to preserve a certain amount of proteins needed for bone formation during demineralisation [13]. However, in the process of demineralisation there occurs a reduction of density and strength of the implant, the requirements for which are due to its type and application, causing the need for monitoring the level of residual implant mineralisation.

Raman spectroscopy was proposed for estimating the ratio of mineral and organic components of bone tissue as a function of demineralisation time under conditions of laboratory transplantology, in biotechnological cell and tissue engineering and in experimental medicine. The aim of this study is to determine the ratio of mineral and organic components of donor bone biomaterial during the engineering of bone grafts based on the analysis of the Raman spectra.

2. Materials and methods

2.1. Research objects

As objects of study we used samples of bone tissue of rats and rabbits with varying degrees of mineralisation, as well as a three-dimensional bioplastic material, i.e., demineralised spongy crumb of a series 'Lioplast'® (TU-9398-001-01963143-2004), which is a fine-pored natural bioplastic material and consists of components of only allogeneic cancellous human bone tissue. The first step in the technological process of preparation of such bioimplants was degreasing and complete removal of all elements of bone marrow and blood from bone scaffolds by brief low-frequency ultrasonic treatment (24–40 kHz for two to three minutes).

Then, to obtain a demineralised bone biomaterial, we placed bone tissue in a 1.2 N solution of HCl for a time which depends on the location of the bone extraction and donor age. The next step was lyophilisation of the sample on an ALPHA

E.V. Timchenko, P.E. Timchenko, L.A. Taskina Samara State Aerospace University (National Research University), Moskovskoe shosse 34, 443086 Samara, Russia; e-mail: Vorobjeva.82@ mail.ru, Timpavel@mail.ru, retuo@mail.ru, zakharov@ssau.ru;
L.T. Volova, Yu.V. Ponomareva Institute of Experimental Medicine and Biotechnology, Samara State Medical University, ul Gagarina 20, 443079 Samara, Russia; e-mail: csrl.sam@mail.ru

Received 9 April 2014; revision received 15 June 2014
Kvantovaya Elektronika **44** (7) 696–699 (2014)
Translated by I.A. Ulitkin

2-4 LSC freeze-dryer. Rabbit bone was also treated by this technology. Nondemineralised samples were obtained by excluding the stage of demineralisation in a hydrochloric acid solution from the preparation process.

2.2. Experimental setup

Spectral characteristics of the samples were studied by using the experimental setup (Fig. 1), which includes a digital, high-resolution Shamrock sr-303i spectrograph with an integrated, cooled ANDOR DV420A-OE CCD camera, an RPB785 Raman fibre-optic probe combined with a LuxxMaster LML-785.0 RB-04 laser module (adjustable power up to 500 mW, wavelength of 785 nm). Due to the low level of autofluorescence this wavelength is well-proven of all the wavelengths of the visible range in Raman spectroscopy in biological applications. The 500 mW output of the laser causes no destructive changes in the samples within the exposure times up to 50 s.

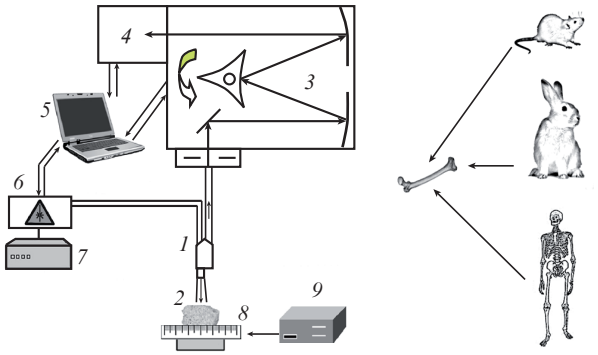

Figure 1. Experimental setup: (*1*) Raman probe; (*2*) object; (*3*) spectrograph; (*4*) CCD camera; (*5*) computer; (*6*) laser module; (*7*) laser power supply module; (*8*) stepper motor-driven translation stage; (*9*) control unit of the translation stage.

The Raman probe (*1*) focuses the laser light on the object (*2*) at a distance of 7.5 mm from the exit window (focal spot diameter of 0.2 mm) and collects both autofluorescence radiation and scattered radiation. The in-built wideband filter of the probe (*1*) is designed to separate radiation in the spectral range 790–1200nm, which is then sent to the spectrograph (3) with an integrated CCD camera (*4*) through the optical fibre. For noise reduction the camera (*4*) is cooled down to –60 °C, providing a spectral resolution of 0.15 nm (~1 cm^{-1}). A stepper motor-driven translation stage (*8*) allows the sample to be spatially scanned.

Isolation of the Raman spectrum against the autofluorescence background was carried out by polynomial approximation [14, 15] of the recorded spectra.

3. Results

Figure 2 shows typical spectra of different types of donor bone tissues (rat, rabbit and human). The registered Raman bands correspond to vibrational modes [16, 17] listed in Table 1. One can see that these Raman lines are present in all types of tissue samples. The most significant difference manifests itself in the 855 and 876 cm^{-1} bands of proline and hydroxyproline, which are a part of collagen and have the largest value in the case of samples of human bone tissue.

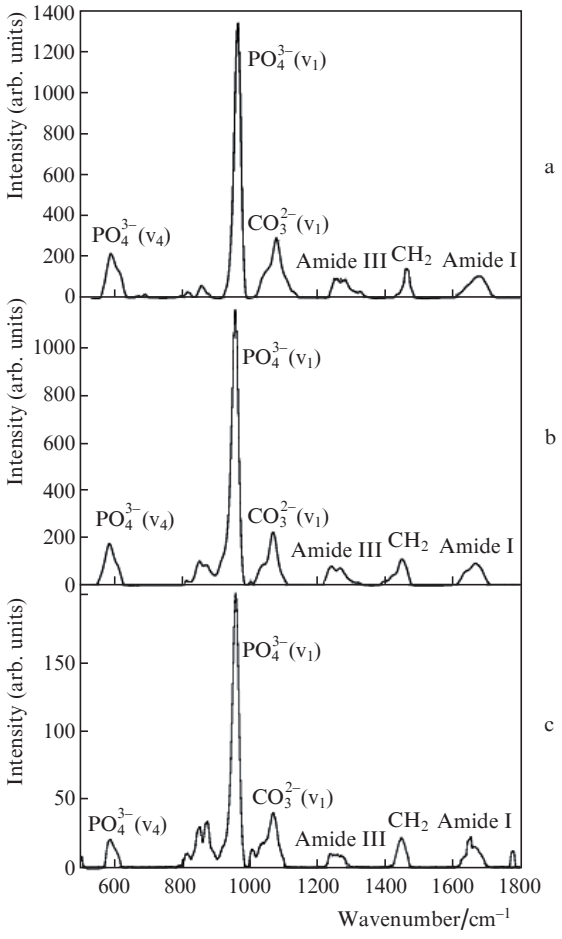

Figure 2. Raman spectra of the samples of nondemineralised bone tissue of (a) rat, (b) rabbit and (c) human.

Kiseleva [16] studied the peculiarities of the Raman spectra of human bone tissue samples during the development of arthrosis, leading to a decrease in the relative content of B-type carbonate ions in the hydroxyapatite structure. Following this work, we have determined the degree of demineralisation by a ratio of intensities of Raman bands of PO_4^{3-} and amide I. Then, for the quantitative determination of the degree of leaching of organic components in the process of demineralisation we can introduce a mineral/organic matrix ratio, which is the ratio of the intensities of peaks in

Table 1. Raman bands for bone tissue [16].

Wavenumber/cm^{-1}	Fragment, vibration
580	PO_4^{3-} (v_4) (P–O, deformation)
855	Benzene ring of proline
876	Benzene ring of hydroxyproline
950–962	PO_4^{3-} (v_1) (P–O, symmetric stretching)
1001–1003	'Breathing' mode of benzene ring of phenyl alanine
1030	PO_4^{3-} (v_3) (P–O, asymmetric stretching)
1045	PO_4^{3-} (v_3) (P–O, asymmetric stretching)
1065–1070	CO_3^{2-} (v1) B-type substitution (C–O planar stretching)
1245–1270	Amide III (C–N–H, stretching)
1445	CH_2 (deformation torsional)
1610–1620	Y8a (vibrations of tyrosine side chains
1665	Amide I (C–N–H, stretching)

the 950–962 cm^{-1} region (oscillation of PO_4^{3-}) and in the 1665 cm^{-1} region (absorption band of amide I):

$$M = I_{PO_4^{3-}}/I_{\text{amide I}}. \quad (1)$$

A peak intensity ratio in the regions of 1065–1070 and 950–962 cm^{-1} (the carbonate/phosphate ratio) can be used to identify a donor material with osteoarthritis:

$$K = I_{CO_3^{2-}}/I_{PO_4^{3-}}. \quad (2)$$

We have preliminary determined the sensitivity of the technique to the height of the probe over the object of study and the time of exposure to the laser source. We have found that in the case of prolonged exposure (80 min), the intensity increases by 6%–8% and saturates while preserving the shape of the spectral curve, which is apparently due to a change in fluorescence intensity upon heating. The maximum integrated intensity of light detected by the spectrograph is observed at a height of 7 mm. However, changing the distance from the probe to the object from 6 to 8 mm has little effect on the values of the coefficients K and M: the measurement error did not exceed 3%.

The relative concentration of organic substances of demineralised bone material can be estimated from the intensity of the following bands: the absorption band of amide III (1245–1270 cm^{-1}), the deformation torsional vibration band of CH_2 (1445 cm^{-1}) and the 1610 cm^{-1} region corresponding to the vibration of the side chain of tyrosine [16].

Figure 3a shows the Raman spectra of bone samples taken from different sites (for comparison, the nondemineralised sample was also subjected to degreasing and drying).

For a bone with a cartilaginous tissue, as compared with the central part of femur (Fig. 3a), we observed a decrease in the intensity of the 956 cm^{-1} band at a significant increase in the intensity of the peaks corresponding to the vibration of the benzene ring of proline (855 cm^{-1}), hydroxyproline (876 cm^{-1}) and CH_2 vibration. Figure 3b shows the Raman spectra of the native (with elements of muscle tissue and blood) donor bone biomaterial (rat). In the presence of aggregates of blood cells on the surface of bone, additional peaks appear in the regions of 600–850 and 1080–1200 cm^{-1}.

In addition to the quality of treatment of donor material implants, quite essential is difference in the M values for different donors (Table 2) (averaged over the five samples and five points).

As seen from Table 2, the values of M for the human and rabbit are maximal and equal to 10.9–10.8 for the selected samples. Due to the difficulty of extraction of the cancellous bone fraction in the rat, we used in the experiments whole femur, wherein the ratio of M is 10% less than that of nondemineralised human bone tissue. At the same time, for the same exposure times in a demineralised solution, the value of M for the rat femoral bone was higher (0.89) than the rabbit and human femoral cancellous bone fraction (0.54–0.63).

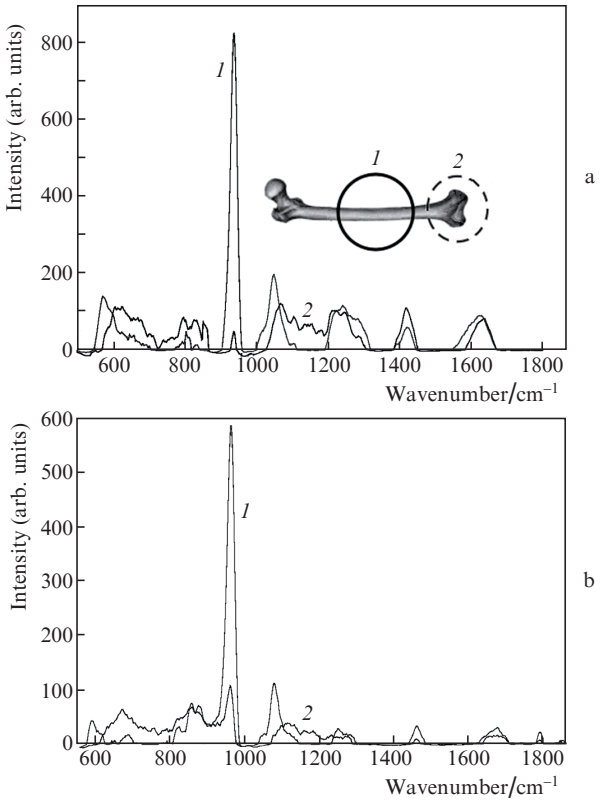

Figure 3. Raman spectra for (a) nondemineralised and (b) native samples of femur; (*1*) central part, (*2*) section with cartilaginous plate.

This is due to the higher density and lower porosity of the rat bone biomaterial and should be taken into account in the process of demineralisation.

The donor material is characterised by variation in the parameters, which can be caused by individual characteristics of organisms, age of the donors and various diseases. To assess the natural spread in the donor tissue parameters, we measured the ratios of M and K for bone tissue (femur), taken from six rats of one group but extracted on different days during the month (Fig. 4).

For this sampling the natural spread in the M ratio was 65% for nondemineralised samples and about 20% for demineralised ones, and the spread in the K ratio for nondemineralised samples was equal to 35%, which is much higher than the error of their determination and is due to the spatial inhomogeneity of bone mineral density. In selecting the demineralisation regimes it is necessary to take into account the natural fluctuations of the primary donor material; otherwise, the spread in the prepared implant parameters reaches about 20% (Fig. 4). For each donor the demineralisation duration will differ from individually selected time of storage in the acid (depending on the initial parameters of the material).

Table 2. Ratio of mineral/organic matrix for bone tissue samples from different donors.

State of tissue	Sample		
	Human femoral cancellous bone fraction	Rabbit femoral cancellous bone fraction	Rat femur
Nondemineralised	10.9 ± 0.2	10.9 ± 0.2	9.1 ± 0.2
Demineralised	0.54 ± 0.02	0.63 ± 0.02	0.89 ± 0.02

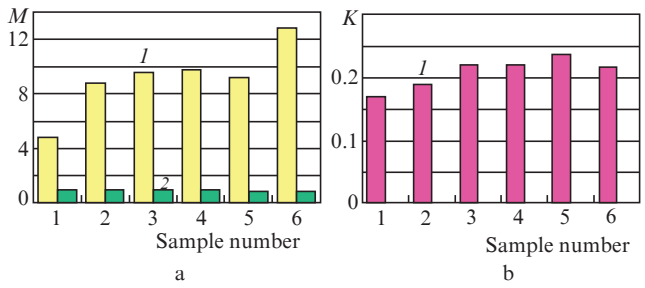

Figure 4. Histograms of (a) mineral/organic matrix and (b) carbonate/phosphate ratios for the femur samples of six rats; (*1*) nondemineralised tissue and (*2*) demineralised tissue.

Figure 5 shows the Raman spectra of the samples of nondemineralised and demineralised rabbit femoral cancellous bone fraction. For all three samples the most informative are the bands of 956 cm^{-1} [$RO_4^{3-}(v_1)$] and 1065–1070 cm^{-1} [$CO_3^{2-}(v_1)$]. In the demineralised cancellous bone tissue we observed a sharp decrease in the intensity of the peak at 956 cm^{-1}: by 86% during five-minute demineralisation and by 98% during twenty-minute demineralisation. A similar decrease was observed in the 1065–1070 cm^{-1} band, followed by the emergence of the 1079–1090 cm^{-1} band corresponding to the hydrated amorphous state of CO_3^{2-} [18]. During the analysis of the spectra we found that the intensity of the band, which is responsible for the 'breathing' mode of the benzene ring of phenylalanine (1003–1005 cm^{-1}), decreases with increasing demineralisation duration.

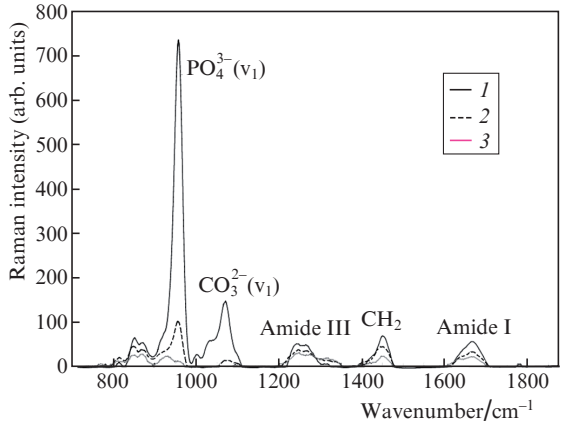

Figure 5. Comparison of the Raman spectra of the samples of bone tissue: (*1*) nondemineralised sample, (*2*) sample demineralised for 5 min and (*3*) sample demineralised for 20 min.

4. Conclusions

We have measured the Raman spectra of bone biomaterial with varying degrees of demineralisation for three types of donors, i.e., rat, rabbit and human. It is shown that the process of demineralisation can be quantitatively controlled by using the intensity ratios of Raman spectral peaks, which are proportional to the mineral/organic matrix and carbonate/phosphate ratios. Thus, after five-minute demineralisation of spongiosis in a 1.2 N hydrochloric acid solution the mineral/organic matrix ratio is reduced by 86%, and after twenty minutes – by 98%.

For each donor the duration of demineralisation should be selected individually. Consequently, the optical method for the certification of implants by the spectral ratios of *K* and *M* may provide a substantial reduction in the spread of the output parameters, and hence improve the consumer qualities of the implants as a result of customisation of duration of their treatment.

References

1. Grin' V.K., Papandopulo A.G., Shtutin A.A., Gnilorybov A.M., Miminoshvili O.I., Fistal' E.Ya., Mikhailichenko V.Yu. *Vestnik Neotlozhnoi i Vosstanovitel'noi Meditsiny*, **13** (1), 3 (2012).
2. Mobini S., Solati-Hashjin M., et al. *J. Med. Biol. Eng.*, **33** (2), 207 (2011).
3. West P.A., Torzilli P.A., Chen C., Lin P., Camacho N.P. *J. Biomed. Opt.*, **10** (1), 014015 (2005).
4. Kirilov I.A. *Khirurgiya Pozvonochnika*, **3**, 105 (2004).
5. Urist M.R., Iwata H.J. *Theor. Biol.*, **38**, 155 (1973).
6. Savel'ev V.I., Khlebovich N.V., in *Nauchnye Trudy St. Peterburgskogo Politekhnicheskogo Universiteta* (St. Petersburg, 1993) p. 125.
7. Slutskii L.I., Sevast'yanova N.A. *Ortopediya i Travmotologiya*, **8**, 82 (1986).
8. Zakharov V.P., Belokonev V.I., Bratchenko I.A., Timchenko P.E., Ponomareva Yu.V., Vavilov A.V., Volova L.T. *Kvantovaya Elektron.*, **41** (4), 318 (2011) [*Quantum Electron.*, **41** (4), 318 (2011)].
9. Bonewald L.F., Harris S.E., Rosser J., Dallas M.R., Dallas S.L., Camacho N.P., Boyan B., Boskey A. *Calcif. Tiss. Int.*, **72**, 537 (2003).
10. Stanford C.M., Jacobson P.A., Eanes E.D., Lembke L.A., Midura R.J. *J. Biol. Chem.*, **270** (16), 9420 (1995).
11. Otto C., de Grauw C.J., Duindam J.J., et al. *J. Raman. Spectr.*, **28** (2–3), 143 (1998).
12. Tarnowski C.P., Ignelzi M.A., Morris M.D. *J. Bone Mineral Res.*, **17**, 1118 (2002).
13. Zhao J. et al. *Soc. Appl. Spectros.*, **61** (11), 1225 (2007).
14. Zakharov V.P., Larin K.V., Kozlov S.V., Moryatov A.A., Bratchenko I.A., Myakinin O.O., Artem'ev D.N., Khristoforova Yu.A. *Fizika Volnovykh Protsessov i Radiotekhnicheskie Sistemy*, **16** (3), 73 (2013).
15. Timchenko P.E., Zakharov V.P., Volova L.T., Boltovskaya V.V., Timchenko E.V. *Komp'yuternaya Optika*, **35** (2), 183 (2011).
16. Kiseleva D.V. *Ezhegodnik Trudov IGG UB RAS*, **157**, 332 (2010).
17. Morris M.D., Finney W.F. *IOS Press – Spectros.*, **18**, 155 (2004).
18. Wehrmeister U., Jacob D.E., Soldati A.L., Loges N., Hagerb T., Hofmeisterb W. *J. Raman Spectros.*, **42**, 926 (2011).